



ISSN: 0975-833X

Available online at <http://www.journalcra.com>

International Journal of Current Research
Vol. 10, Issue, 04, pp.68354-68360, April, 2018

INTERNATIONAL JOURNAL
OF CURRENT RESEARCH

RESEARCH ARTICLE

SYNTHESIS AND CHARACTERIZATION OF ZEOLITE LINDE TYPE L AND ITS APPLICATION IN ORGANIC SYNTHESIS

*Adya Jain, Shikha Singh, Kautily Rao Tiwari, Neeraj Kumar and Radha Tomar

S. O. S. in Chemistry, Jiwaji University, Gwalior, M.P., 474011, India

ARTICLE INFO

Article History:

Received 05th January, 2018

Received in revised form

24th February, 2018

Accepted 08th March, 2018

Published online 30th April, 2018

Key words:

Zeolite LTL, Hantzsch Condensation, Dimedone, 9, 10-Diarylacridine-1, 8- Dione.

ABSTRACT

This protocol deals with novel method for the synthesis and characterization of Zeolite Linde type- L by hydrothermal method using PTFE-lined stainless steel autoclave. The synthesized zeolite LTL was used as catalyst for the Hantzsch reaction mechanism for the synthesis of Acridine-1, 8- dione derivatives. Efficiency of Zeolite-LTL has been observed at various parameters (i.e. different solvent, temperature, catalyst concentration, time interval and catalytic recycling) over the percentage yield of various derivatives. Synthesis of 9, 10-Diarylacridine-1, 8-dione was carried out by single-pot Hantzsch condensation reaction, which includes three component reactants i.e. aldehyde, amine and 5, 5-Dimethyl-1, 3- cyclohexanedione (dimedone). Expeditious with excellent Yield of synthesized drug intermediates from H-LTL was found to be 98.88% in ethanol at 90°C. The synthesized zeolites sample were characterized by the help of FT-IR, XRD, BET Surface Area Analysis and SEM while the synthesis of drug derivatives were confirmed by FT-IR, ¹H-NMR and LC-MS.

Copyright © 2018, Adya Jain et al. This is an open access article distributed under the Creative Commons Attribution License, which permits unrestricted use, distribution, and reproduction in any medium, provided the original work is properly cited.

Citation: Adya Jain, Shikha Singh, Kautily Rao Tiwari, Neeraj Kumar and Radha Tomar. 2018. "Synthesis and Characterization of Zeolite Linde Type L and its application in organic synthesis", *International Journal of Current Research*, 10, (04), 68354-68360.

INTRODUCTION

The employment of catalyst greatly enhances the yield percentage and purity of drug molecules therefore fulfills the need of worldwide demands for pharmaceutical medicines. Zeolite exclusive advantages as catalysts include less or noncorrosive nature, no waste or disposal problem, abundance, low cost, high thermo stability, great adaptability to practically all types of catalysis, heterogeneous i.e. easily separable from reaction mixture, great acid strength, easier scale up for continuous processes, etc. Zeolite LTL exhibit excellent catalytic properties on account of its unique structural and compositional features. The framework of zeolite LTL, a wide pore size zeolite, is based on polyhedral cages formed by five six-membered and six four-membered rings (Taborda, 2001; Modhera, 2009; Jentoff, 1998). The main channels consisting of alternate cancrinite cages and hexagonal prisms form columns that run parallel to the c-axis. Each channel is isolated from all neighboring ones (Barrer, 1969; Van Steen, 2004; Weitkamp, 1999; Hantzsch, 1881). Very few literatures has been reported for zeolite Linde Type L as catalyst for drug delivery. The oldest, and perhaps most important, of the classical synthesis of pyridines is the Hantzsch (dihydro) pyridine synthesis described by Arthur Hantzsch (Hantzsch, 1881).

*Corresponding author: Adya Jain,

S. O. S. in Chemistry, Jiwaji University, Gwalior, M.P., 474011, India.

Dihydropyridine (DHP) derivatives (i.e. Acridinediones, quinolines) displays wide array of biological activities such as vasodilator, anti-atherosclerotic, antitumor, antidiabetic (Shan, 2004) calcium LTL-blockers, antihypertensive activity, α 1a-antagonists and heart defibrillation. Acridine derivatives possess number of biological activities i.e. antitumor (Mikata, 1998), cytotoxic, anticancer (Venkatesan, 2008), antimicrobial, anti multidrug resistant, fungicidal, antibacterial activity, antiglucoma (Ulus, 2013), mutagenic properties etc. Dihydropyridine molecules are synthesized by one pot multicomponent condensation reaction i.e. Hantzsch Condensation Reaction which is a catalytic driven reaction. In the absence of catalyst, the obtained yield percentage is unsatisfactorily in lower amount and the reaction completes in long duration. Different mechanisms for the synthesis of Dihydropyridine derivatives has been reported by using various catalysts and solvents including alumina (neutral or basic) as mineral solid supports using DMF as solvent (Suarez, 1999), *p*-dodecylbenzenesulfonic acid (DBSA) as a Bronsted acid-surfactant-combined catalyst (Jin, 2004), Amberlyst-15 in CH₃CN (Das, 2006), 1-butyl-3-methyl-imidazolium tetrafluoroborate ((bmim)(BF₄)) (Fan, 2007), tris(pentafluorophenyl) borane (B(C₆F₅)₃) (Chandrasekhar, 2008), *L*-proline (Venkatesan, 2009), sodium 1-dodecanesulfonate (SDS) (Shi, 2009), Brønsted acidic imidazolium salts containing perfluoroalkyl tails (Shen, 2009) Hf(NPf₂)₄ (Hong, 2012), nano-Fe₃O₄ (Ghasemzadeh, 2012),

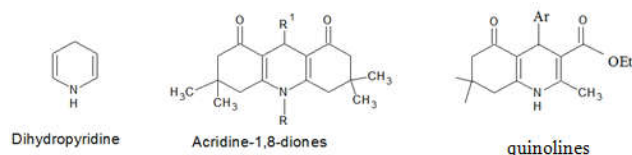


Fig 1. Structures representing Parent Nucleus Molecule and Drug Derivatives

Cross-dehydrogenative regioselective Csp^3-Csp^2 coupling of enamino-ketones (Sarkar, 2016), (Bmim)ClO₄ (Makone, 2015), aluminium dodecyl sulfate trihydrate (Al(DS)₃·3H₂O a Lewis acid-surfactant-combined catalyst (Hasaninejad, 2015), magnetite (Fe₃O₄)/chitosan as a magnetically recyclable heterogeneous nanocatalyst (Maleki *et al.*, 2015), P₂O₅ (Nalini, 2013), ionic liquid triethylamine hydrogen sulphate (Et₃N)⁺(HSO₄)⁻ (Rajendran *et al.*, 2012), monodisperse platinum nanoparticles supported with reduced graphene oxide (Aday *et al.*, 2016) etc. However, above these methods have some limitations such as formation of long reaction time (generally from 3 h to even 24 hrs), high temperature, strong acidic condition leading corrosive and high toxicity, low yield and expensive reagents.

Experimental

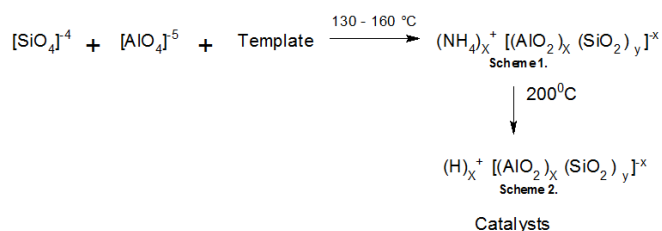
Synthesis of Zeolite as Catalysts

Synthesis of Zeolite LTL

In a 250 ml round bottomed flask a mixture of 12.5 ml distilled water, 7.59 g KOH and 3.955 g alumina were prepared which was heated until a clear solution is obtained. After cooling, 37.56 g silica sol, 30.75 ml distilled water and 3.875 g Mg(NO₃)₂ were mixed until homogeneous solution is obtained. The mixture was kept in a PTFE-lined stainless steel autoclave and heated in oven at 175°C for 48 h. Thereafter obtained mixture was filtered and dried in oven at 150°C for 16 h.

Conversion of K-LTL to H-LTL

In a 250 ml round bottomed flask, 9 g of zeolite (Na form), 7.230 g NH₄Cl and 13.80 ml distilled water mixed with 0.1M HCl solution to maintain pH= 4 of the solution. This reaction mixture was stirred for 30 min at 60°C. Thereafter obtained material was washed and filtered by double distilled water. Finally precipitate was dried in oven at 60°C for 24 h. Further the powdered mixture was calcinated at 200°C for 60 min. so that ammonia gets converted to NO₂ (↑) leaving H-form zeolite.



Scheme 1 and 2. Synthesis and Modification of Zeolite

Synthesis of 1,8-Acridinedione derivatives (3,3,6,6-Tetramethyl-3,4,6,7,9,10-hexahydro-1,8-acridinedione)

In ethanol (solvent), Primary amine (1 mmol) was added to the mixture of 5, 5-dimethyl-1,3-cyclohexanedione (dimedone) (2 mmol), an aromatic aldehyde (1 mmol) and zeolite (0.1 g) at

90 °C (Fig. 2) by using refluxing water. Reaction completion was realized by Thin Layer Chromatography. The reaction mixture was filtered and the product was obtained as filtrate, collected and dried at room temperature. The purification of solid residue was performed by recrystallizing from ethanol to obtain pure 1, 8-dioxo-decahydroacridine derivative form. The synthesized compound was characterized by the help of FTIR, LC-MS and ¹H-NMR.

$$\text{Product yield (\%)} = \frac{\text{Actual yield (g)}}{\text{Theoretical yield (g)}} \times 100\%$$

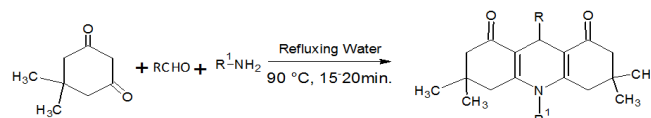


Fig. 2. One Pot Hantzsch Condensation Reaction

Synthesis of 9, 10-Diarylacridine-1, 8-dione was carried out by single-pot Hantzsch condensation reaction, which includes three component reactant molecule i.e. aldehyde, amine and 5, 5-Dimethyl-1, 3- cyclohexanedione (dimedone) having 1:1:2 proportion respectively. Plausible mechanism for Hantzsch pathway can be explained, as it is a combination of Aldol condensation and Michael addition. Reaction initiates by Aldol condensation between aldehyde and one dimedone molecule to form Ist Intermediate which further undergoes Michael addition by reacting with another molecule of dimedone. Finally aniline molecule reacts with the intermediate by dehydration rearrangement to form Dihydropyridine drug intermediate.

RESULT AND DISCUSSION (I)

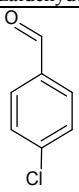
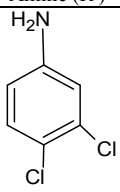
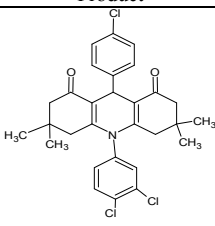
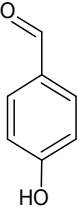
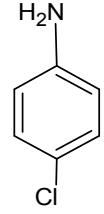
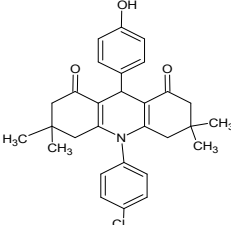
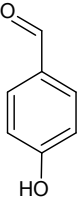
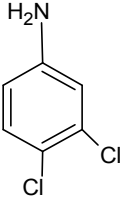
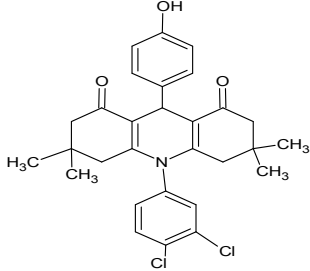
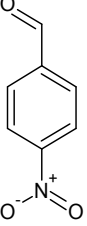
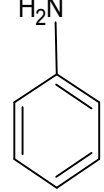
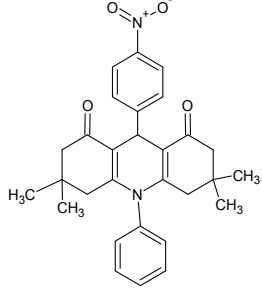
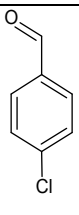
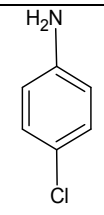
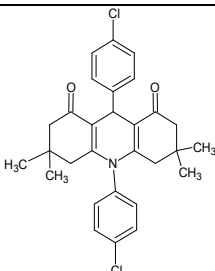
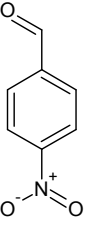
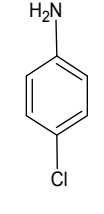
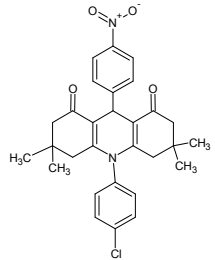
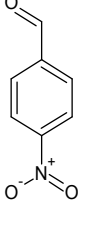
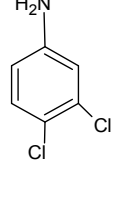
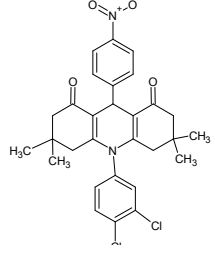
Melting points were determined in open capillaries from melting point instrument. All solvents and chemicals were purchased from E. Merck, Sisco and Qualigens. All solvents used were dried and distilled according to standard procedures. Infrared spectra of the synthesized drug intermediates and zeolites were recorded by “Spectrumto-Perkin Elmer” spectrophotometer in the range of 4000–400 cm⁻¹ by using KBr pellets (200:1). The Powder X-Ray diffraction spectra were recorded by using “Miniflex 600” Diffractometer operated at voltage of 40 kV and a current of 30mA with Copper K_α radiation in a θ- 2θ configuration with a goniometer speed of 2°/min and a step of 0.02° in the 2θ range scanning from 5° to 90° for synthesized zeolites samples.

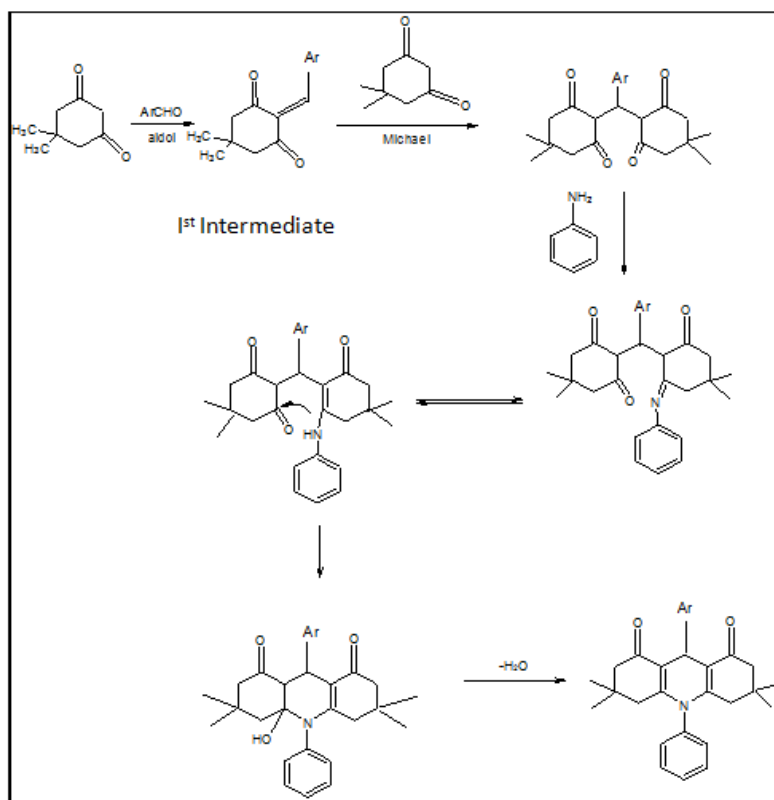
¹H-NMR spectra were determined in DMSO-d₆ solvent by the help of JEOL-JNM-ECA Series (Delta V4.3)-400 MHz-FT-NMR. Data for ¹H NMR are reported as follows: chemical shift, integration, multiplicity (s = singlet, d = doublet, t = triplet, q = quartet, m = multiplet) and coupling constants. BET surface area and porosity of zeolite samples was determines by using “Gemini VII 2390 Surface Area Analyzer (Micromeritics)”. BJH adsorption and desorption cumulative surface area of pores has been measured between 17.000 Å⁰ and 3000.000 Å⁰ widths. Analytical thin layer chromatography was performed using 0.25 mm silica gel plates (Ethyl Acetate: n-Hexane:: 3:1). Mass spectroscopy was recorded by Shimadzu “LC-MS 8030 Spectrometer”.

Fourier Transform Infrared Spectroscopy

The finger print region of FT-IR determines the formation of zeolite.

Table 1. Synthesis of Different derivatives of 1, 8-Acridinedione:

S.No.	Benzaldehyde (R)	Amine (R')	Product	Yield (%)	M.P. (°C)
1.				94.29	244-245
2.				98.79	238-240
3.				98.88	220-225
4.				97.43	245-247
5.				95.82	284-287
6.				93.12	280-283
7.				92.27	277-280



Scheme 3. Plausible mechanism for the formation of 1,8-Acridinedione

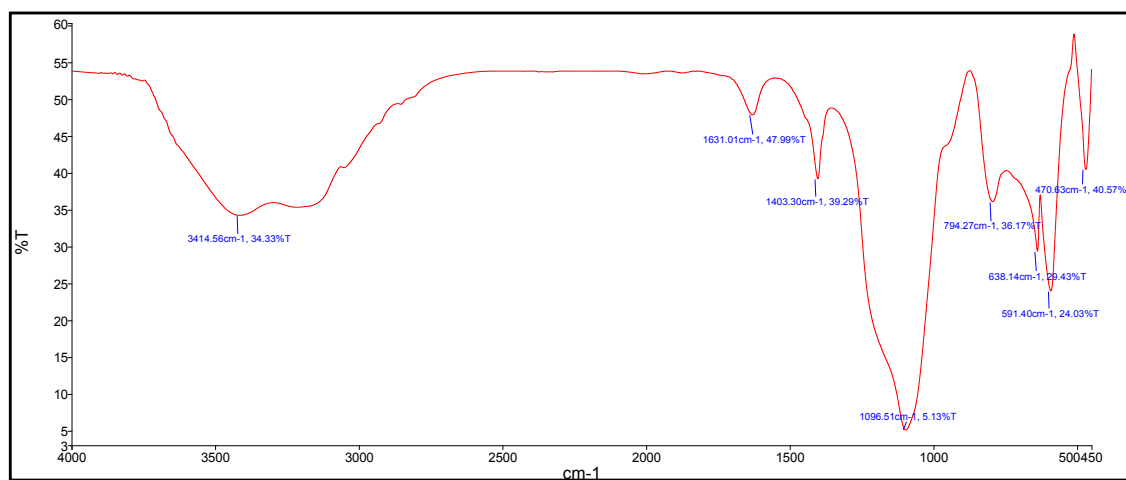


Fig 3. FT-IR spectra of H-LTL

FTIR spectrum of calcined zeolite shows adsorption bands at 450 cm^{-1} which attributes to Si, Al-O band vibrations while those around 1000 cm^{-1} and 750 cm^{-1} are due to symmetric and anti-symmetric stretches of zeolite framework. The stretching vibration of SiO_4 are shifted towards lower frequency indicating that the presence of the internal $\text{Si-O}\cdots\text{HO-Si}$ bonds.

Scanning Electron Microscope

The SEM micrograph of nanoporous zeolite shows the interconnection of porous structure by agglomerating of nanoparticles on H-LTL with an average particle size less than between $2\text{--}10\ \mu\text{m}$. (Lee *et al.*, 2012). However small variations may be observed in the SEM images of zeolite which is due to the presence of deposition of metal salts and organic part of ammonium salt used during the synthesis of H-form Zeolite on zeolite surface.

X-Ray Diffraction

The X-Ray Diffraction pattern shows the crystalline phase of zeolite without any amorphous phase. From the diffraction signals, the sharp peaks at 2θ value corresponding to 25.16° for zeolite-H-LTL, which are clearly observed. Generally sharp peaks determine the crystalline nature of material.

BET Analysis

The BET surface area of zeolite LTL was found to be: $24.2013\text{ m}^2/\text{g}$, Langmuir surface area: $36.9077\text{ m}^2/\text{g}$, BJH desorption cumulative surface area of pores between 17.000 \AA^0 and 3000.000 \AA^0 widths: $29.025\text{ m}^2/\text{g}$, BJH Desorption cumulative surface area of pores between 17.000 \AA^0 and 3000.000 \AA^0 widths: $32.4035\text{ m}^2/\text{g}$.

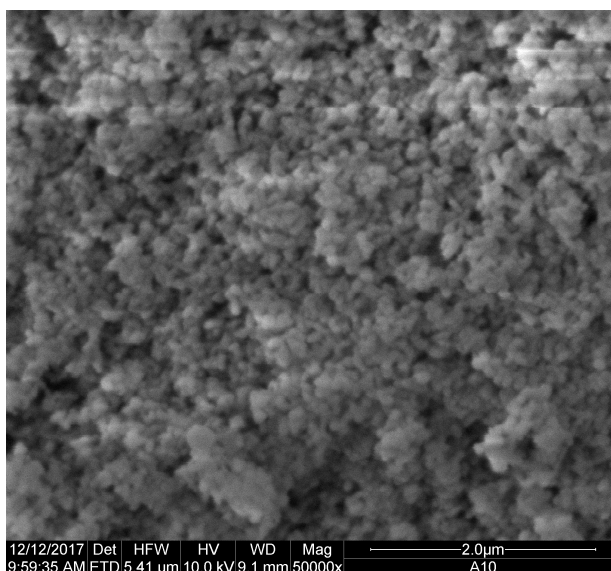


Fig 4. SEM micrograph of Nanoporous Zeolite H-LTL

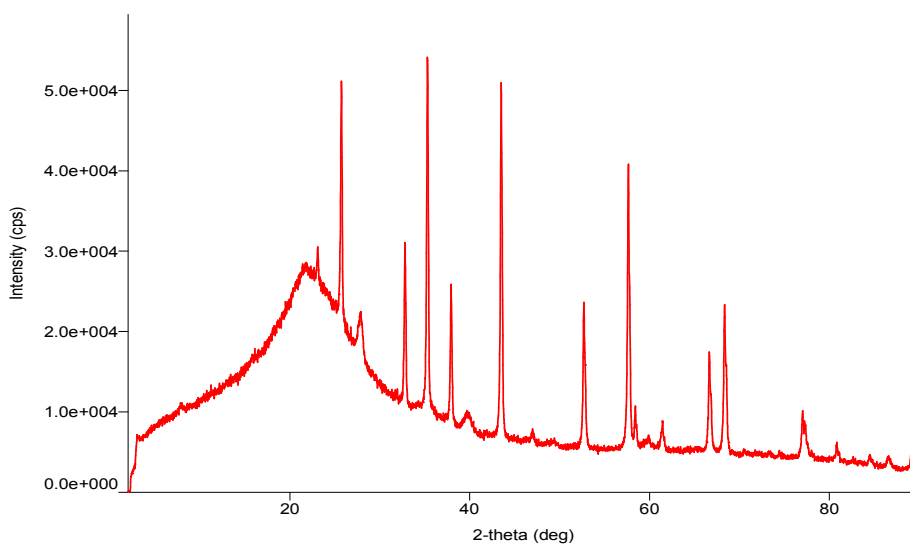


Fig. 5. XRD of H-LTL

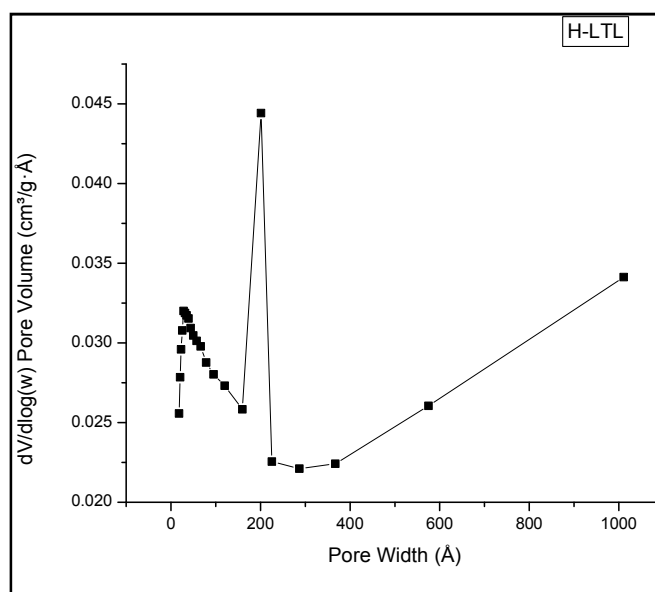
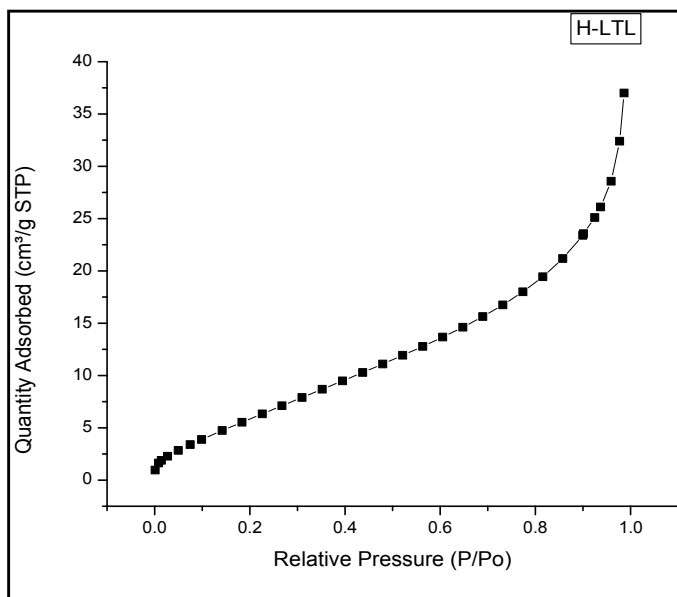


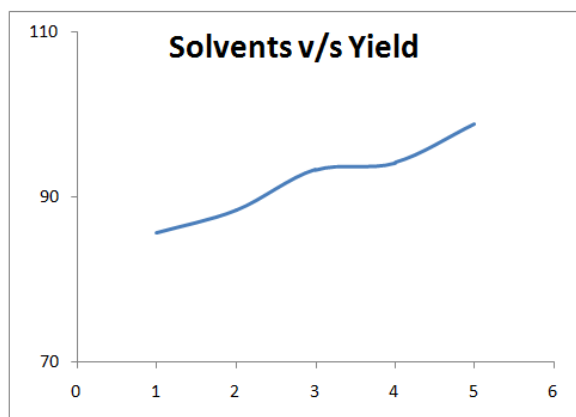
Fig 6 and 7. BET analysis representing Relative Pressure v/s Quantity Adsorbed and Pore width v/s Pore volume

RESULT AND DISCUSSION (II)

This model reaction has been standardized by using Zeolite LTL as catalysts, various solvents, amount of catalyst and reaction conditions based on different temperatures and time intervals. Firstly the effect of the solvent has been investigated on the model reaction as shown in Table 2. The model reaction was performed in various solvent such as CHCl_3 , CH_3CN , Dioxane, Ethanol, Toluene under the same reaction conditions. The experimental results show highest yield% in ethanol in shortest reaction period rather than other solvent used. Also, ethanol is polar protic solvent which favors the reaction conditions i.e. acidic medium and superior due to its environmental friendly property. Table 3 and Table 4 represent reaction yield at various temperature and time intervals. Excellent yield% were observed after 60 min at 90°C keeping all reaction conditions in hand (0.05g catalyst and ethanol as solvent).

Table 2, Graph 1: Studying the yield of 9-(4-OH C_6H_5)-10-(3, 4- $\text{Cl}_2 \text{C}_6\text{H}_3$)-3, 3, 6, 6-Tetramethyl acridine-1, 8-dione (6) from different solvents

Solvent	% yield of catalytic forms
	H-LTL
Acetonitrile	85.60
Toluene	88.35
Chloroform	93.26
1,4-Dioxane	94.13
Ethanol	98.88



All reactions were carried out at 90°C from 30-40 min. with catalyst H- β amount of 0.05 g. Amount of catalyst is another important parameter in terms of reaction efficiency. Reaction in the absence of catalyst shows only 15% yield. Total 10 sets of reaction were employed keeping all reaction conditions constant with varying catalyst amount from 0.01 to 0.10 g. It was found that with increase in the amount of catalyst, product yield increases upto certain limit after which it remains constant.

Table 3, Graph 2: Studying the yield of 9-(4-OH C_6H_5)-10-(3, 4- $\text{Cl}_2 \text{C}_6\text{H}_3$)-3, 3, 6, 6-Tetramethyl acridine-1, 8-dione (6) at different temperature

Temperature ($^\circ\text{C}$)	% yield of catalytic forms
	H-LTL
0	11.90
30	27.31
60	54.09
90	98.88
120	67.29

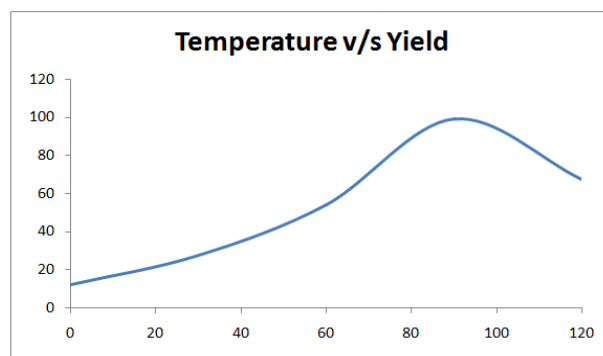
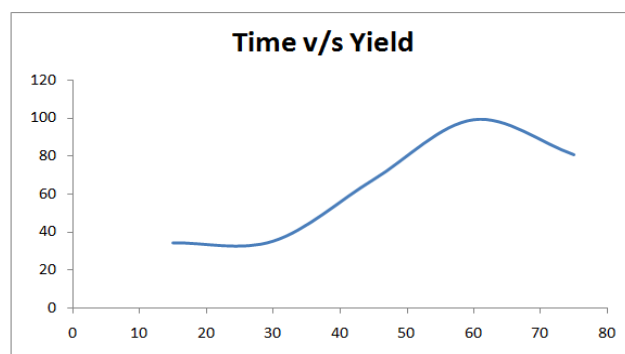


Table 4, Graph 3: Studying the yield of 9-(4-OH C_6H_5)-10-(3, 4- $\text{Cl}_2 \text{C}_6\text{H}_3$)-3, 3, 6, 6-Tetramethyl acridine-1, 8-dione (6) at different time

Time (min.)	% yield of catalytic forms
	H-LTL
15	34.16
30	33.09
45	67.41
60	98.88
75	80.49



This occurs due to increase in active sites upto certain limit. After further increase in catalyst, the additional acid sites cause no effect because the reagents may loss sufficient sites to bind with. The most essential feature of catalysts depends in its reusability which makes it commercially more usable and cheaper. After the reaction was completed, the catalyst was separated by simple filtration then washed 2-4 times with ethanol and dried in oven over 120°C for 8h. The catalyst was used in several runs without any major loss in their activity. The small change in yield% was due to reduce catalyst structure during recovery process. The basic drawback of filtration is that the product gets attached to the filter paper which is unable to recover thus leading to minor decrease in yield%.

Spectroscopic data of some synthesized drugs

9-(4-Hydroxyphenyl)-3, 3, 6, 6-tetramethyl-10-(4-chlorophenyl)-3,4,6,7,9,10-hexahydroacridine-1, 8-(2H, 5H)-dione: FT-IR (KBr in cm^{-1}) 3883.47, 3055.4, 2999.5, 2850.78, 1718.37, 1488.5, 1517.61, 755.12, 724.33; UV-Vis. λ_{max} – 893.2 nm Absorbance at 0.100 Å; $m/z = 476.5$ (M+H)⁺. ¹H NMR (400 MHz, DMSO- d_6): δ = 0.74 (s, 6 H, 2 CH_3), 0.87 (s, 6 H, 2 CH_3), 1.75 (d, $J = 17.6$ Hz, 2 H, 2 CH), 2.03 (d, $J = 16.0$ Hz, 2 H, 2 CH), 2.18 (d, $J = 16.0$ Hz, 2 H, 2 CH), 2.18 (d, $J = 17.6$ Hz, 2 H, 2 CH), 5.00 (s, 1 H, CH), 7.30 – 7.49 (m, 4 H, ArH), 7.68 (m, $J = 8.8$ Hz, 4 H, ArH), 9.05 (s, 1H, -OH). Anal. Calcd for $\text{C}_{29}\text{H}_{30}\text{ClNO}_3$: C, 73.17; H, 6.35; N, 2.94. Found: C, 73.15; H, 6.24; N, 2.90., $m/z = 476.0$ (M+H)⁺.

9-(4-Hydroxyphenyl)- 3, 3, 6, 6-tetramethyl -10-(3, 4-dichlorophenyl)-3,4,6,7,9,10-hexahydroacridine-1, 8-(2H, 5H)-dione: FT-IR (KBr in cm^{-1}) 3471.47, 3184.5, 2949, 2719.14, 1674.64, 1575, 1460, 1575, 825.5 and 753.56; UV-Vis. λ_{max} – 893.5 nm Absorbance at 0.142 Å; $m/z = 511$ (M+H)⁺. ¹H-NMR (400 MHz, DMSO- d_6): $\delta = 0.72$ (s, 6 H, 2 CH₃), 0.89 (s, 6 H, 2 CH₃), 1.78 (d, J = 17.6 Hz, 2 H, 2 CH), 2.01 (d, J = 16.0 Hz, 2 H, 2 CH), 2.19 (d, J = 16.0 Hz, 2 H, 2 CH), 2.20 (d, J = 17.6 Hz, 2 H, 2 CH), 5.01 (s, 1 H, CH), 7.30–7.49 (m, 4 H, ArH), 7.68 (t, J = 8.8 Hz, 3 H, ArH), 9.05 (s, 1H, -OH). Anal. Calcd for C₂₉H₂₉Cl₂NO₃: C, 68.24; H, 5.73; N, 2.74. Found: C, 68.28; H, 5.05; N, 2.90., $m/z = 510.4$ (M+H)⁺.

9, 10-Bis (4-Chlorophenyl)-3, 3, 6, 6-tetramethyl -3,4,6,7,9,10-hexahydroacridine-1, 8-(2H, 5H)-dione: FT-IR (KBr in cm^{-1}) 3051.84, 2960.17, 2873.28, 1688, 1575.18, 1424.78, 852.7, 762.46; UV-Vis. λ_{max} – 893.5 nm; Absorbance at 0.142 Å; ¹H NMR (400 MHz, DMSO- d_6): $\delta = 0.72$ (s, 6 H, 2 CH₃), 0.89 (s, 6 H, 2 CH₃), 1.89-2.01 (d, J = 16.0 Hz, 2 H, 2 CH₂), 2.42 (d, J = 17.6 Hz, 2 H, CH₂), 5.01 (s, 1 H, CH), 7.30–7.49 (m, 6 H, ArH), 7.68 (d, J = 8.8 Hz, 2 H, ArH). Anal. Calcd for C₂₉H₂₉Cl₂NO₂: C, 70.44; H, 5.91; N, 2.83. Found: C, 70.28; H, 6.05; N, 2.90., $m/z = 494.4$ (M+H)⁺.

9-(4-Chlorophenyl)- 3, 3, 6, 6-tetramethyl -10-(3, 4-dichlorophenyl)-3,4,6,7,9,10-hexahydroacridine-1, 8-(2H, 5H)-dione: FT-IR (KBr in cm^{-1}) 3078.96, 2960, 2887.48, 1718.32, 1587, 1526, 847.72, 738.06; UV-Vis. λ_{max} – 893.6 nm; Absorbance at 0.143 Å; ¹H NMR (400 MHz, DMSO- d_6): $\delta = 0.74$ (s, 6 H, 2 CH₃), 0.91 (s, 6 H, 2 CH₃), 1.89-2.05 (d, J = 16.0 Hz, 2 H, 2 CH₂), 2.43 (d, J = 17.6 Hz, 2 H, CH₂), 5.01 (s, 1 H, CH), 7.35–7.59 (m, 3 H, ArH), 7.58 (d, J = 8.8 Hz, 4 H, ArH). Anal. Calcd for C₂₉H₂₈Cl₃NO₂: C, 65.86; H, 5.34; N, 2.65; Found: C, 65.89; H, 5.35; N, 2.66., $m/z = 528.12$ (M+H)⁺.

Conclusion

The foremost merits of this work are significant and novel due to its competency, environmentally benevolent methodology, reliability, rapidness, recyclable as well as thermally stable zeolite heterogeneous catalytic applicability. Various characterizations (XRD, FT-IR, BET) confirmed the synthesis and structural nanoporous features of Zeolite LTL. Also, the high surface area and greater number of active acid sites are present in H-form Zeolite which favors the model reaction conditions. The reactivity was found highest in ethanol with H-LTL at 90°C for 60 min. i.e. 98.88%. Further the variations in yield of different derivative was observed which was due to the presence of electron withdrawing groups (EWG) and electron donating groups (EDG). Yield of acridine drugs having EWG was found higher than those for having EDG. The main advantages of this protocol are short reaction time, excellent yield, low catalyst loading, high purity of products due to the heterogeneous and harmless properties of Zeolite.

Acknowledgement

I owe to my mentor for supporting and guiding me to make this work possible and Central Instrumentation Laboratory (CIF), Jiwaji University, Gwalior, M.P. for providing necessary instrument support (FT-IR, XRD, LC-MS). I am also thankful to DRDE, Gwalior for providing BET surface area studies and IIT Delhi for ¹H-NMR studies.

Conflict of Interest: All authors owe no conflict of interest.

REFERENCES

- Aday B., Yıldız Y., Ulus R., Eris S., Sen F., Kaya M. 2016. *New J. Chem.*, 40, 748.
- Barrer R. M., Villiger Zeit Krist H. 1969. 128, 352.
- Chandrasekhar S., Rao Y. S., Sreelakshmi L., Mahipal B., Reddy C. R. 2008. *Synthesis*, 11, 1737.
- Das B., Thirupathi P., Mahender I., Reddy V.S., Rao Y. K. 2006. *Journal of Molecular Catalysis A: Chemical*, 247, 233.
- Fan X., Li Y., Zhang X., Qu G., Wang J. 2007. *Heteroatom Chemistry*, 18, 786.
- Ghasemzadeh M. L., Ghomi J. S., Molaei H. C. 2012. *R. Chimie.*, 15, 969.
- Hantzsch A. *Chemische Berichte*, 1881. 14(2), 1637-1638
- Hasaninejad A., Yousefy T., Firoozi S. 2015. *IJST*, 39A2, 129-140.
- Hong M., Xiao G. 2012. *Journal of Fluorine Chemistry*, 144, 7.
- Jentoff R. F., Ysapatsis M., Davis M. F., Gates S.C. 1998. *J. Catal.*, 179, 565-580.
- Jin T. S., Zhang J. S., Guo T. T., Wang A. Q., Li T. S. 2004. *Synthesis*, 2001.
- Lee T. P., Saad B., Ng E. P., Salleh B. 2012. *Journal of Chromatography A*, 1237, 46–54.
- Makone S., Mahurkar S. 2015. *International Journal of Science and Research*, 4 (5), 2493-2496.
- Maleki A., Kamalzare M., Aghaei M. 2015. *J Nanostruct. Chem.*, 5, 95–105.
- Mikata Y., Yokoyama M., Mogami K., Kato M., Okura I., Chikira M; Yano S. 1998. *Inorg. Chim. Acta*, 279, 51–57.
- Modhera B., Chakraborty M., Parikh P. A., Jasra R. V. 2009. *Cryst. Res. Technol.*, 44 (4), 379-385.
- Nalini V., Girija R. 2013. *International Journal of Current Research*, 5(10), 3076-3081.
- Rajendran A., Selvam A., Karthikeyan C., Ramu S. 2012. *Int. J. Cur. Tr. Res.*, 1(1), 24-30.
- Sarkar R., Mukhopadhyay C. 2016. *Org. Biomol. Chem.*, 14, 2706-2715.
- Shan R., Velazquez C., Knaus E. 2004. *J. Med. Chem.*, 47, 254.
- Shen W., Wang L. M., Tian H., Tang J., Yu J. J. 2009. *Journal of Fluorine Chemistry*, 130, 522.
- Shi D. Q., Shi J. W., Yao H. 2009. *Synthetic Commun.*, 39, 664.
- Suarez M., Loupy A., Salfran E., Moran L., Rolando E. 1999. *Heterocycles*, 51, 21.
- Taborda F., Willhammar T., Wang Z., Montes C. 2011. *Zou X. Microporous and Mesoporous Materials*, 143, 196–205.
- Ulus R., Yesildag I., Tanc M., Bulbul M., Kaya M. 2013. *Supuran C. T. Bioorg. Med. Chem.*, 21, 5799–5805.
- Van Steen E., Claeys M., Callana L.H. 2004. Recent Advances in the Science and Technology of Zeolites and Related Materials, Part A: Proceedings of the 14th International Zeolite Conference, Cape Town, South Africa, 25-30th April, Elsevier-Amsterdam.
- Venkatesan K., Pujari S. S., Srinivasan K. V. 2009. *Synthetic Commun.*, 39, 228.
- Venkatesan K., Pujari S. S., Srinivasan K. V. 2008. *Synth. Commun.*, 39, 228–241.
- Weitkamp J., Puppe L. 1999. *Catalysis and Zeolites: Fundamentals and Applications*, Springer-Verlag Berlin Heidelberg.